Comparison of Four Breast Tissue Segmentation Algorithms for Multi-modal MRI to X-ray Mammography Registration

E. García[1(✉)], A. Oliver[1], Y. Diez[2], O. Diaz[1],
A. Gubern-Mérida[3], X. Lladó[1], and J. Martí[1]

[1] Institute of Computer Vision and Robotics, University of Girona, Girona, Spain
egarcia@eia.udg.edu
[2] Tokuyama Laboratory GSIS, Tohoku University, Sendai, Japan
[3] Radboud University Medical Center, Nijmegen, The Netherlands

Abstract. Breast MRI to X-ray mammography registration using patient-specific biomechanical models is one challenging task in medical imaging. To solve this problem, the accurate knowledge about internal and external factors of the breast, such as internal tissues distribution, is needed for modelling a suitable physical behavior. In this work, we compare four different tissue segmentation algorithms, two intensity-based segmentation algorithms (Fuzzy C-means and Gaussian mixture model) and two improvements that incorporate spatial information (Kernelized Fuzzy C-means and Markov Random Fields, respectively), and analyze their effect to the multi-modal registration. The overall framework consists on using a density estimation software (Volpara^{TM}) to extract the glandular tissue from full-field digital mammograms, meanwhile, a biomechanical model is used to mimic the mammographic acquisition from the MRI, computing the glandular tissue traversed by the X-ray beam. Results with 40 patients show a high agreement between the amount of glandular tissue computed for each method.

1 Introduction

Tissue segmentation has been an open problem in medical imaging for decades. In breast imaging, this problem is of particular importance for cancer screening due to the fact that breast density is being established as an important risk factor. Accurate knowledge of the internal tissue of the breast could provide information to radiologist to localize suspicious areas within the breast.

Magnetic Resonance Imaging (MRI), X-ray mammography and Breast Ultrasound are the most common imaging modalities used to early detection and diagnosis of breast diseases in women. X-ray mammography is considered as the gold standard in the early diseases detection. However, the 2D-projection hinders locating suspicious lesions within the uncompressed breast and the sensitivity is limited in women with dense breast. Sometimes, MRI or ultrasound scans are acquired to overcome those issues. In fact, radiologists have found that the combination of these modalities leads to a more accurate diagnosis and management

A. Tingberg et al. (Eds.): IWDM 2016, LNCS 9699, pp. 493–500, 2016.
DOI: 10.1007/978-3-319-41546-8_62

of the breast diseases [11] and researchers have focused their efforts on developing algorithms to fuse the information of the different imaging modalities, taking into account the position of the patient and the loading conditions of the breast during the imaging acquisition [4,8,9].

To fuse the information between MRI and X-ray mammograms, researchers have developed algorithms using patient-specific biomechanical models. During the multi-modal registration process, the biomechanical model is used to mimic the mammographic acquisition, compressing the model and projecting internal tissues from the MRI to a 2D space. However, the limited resolution of the MRI scanner makes almost impossible to get a voxel entirely composed by a single (adipose or glandular) tissue. In this case, the partial volume effect of the voxels must be taken into consideration.

This paper aims to analyze the impact of the tissue segmentation (in particular, of the glandular tissue) during the multi-modal registration. Segmentation algorithms are divided into two categories, parametric, those which assume that the intensity histogram follows a probability distribution (usually the Gaussian distribution), and non-parametric, which classify the voxels using just the intensity of the image, such as K-means or Fuzzy C-means [1].

In our experimental results, first of all, we use the commercial software Volpara^{TM} to extract the glandular tissue from the X-ray mammograms. These obtained density maps are considered as the ground truth of our problem. On the other hand, we use a biomechanical model to mimic the mammographic acquisition from the MRI and to compute the amount of glandular tissue traversed by the X-ray beam at each voxel. Four different segmentation algorithms are used to determine the glandular tissue in the MRI: a Fuzzy C-means (FCM) segmentation and a Gaussian-mixture model provided by the Expectation-Maximization algorithm, and two methods that incorporate spatial prior information to them: the Kernelized Fuzzy C-means and the EM-Markov Random Fields, respectively. Global and local measures are used to quantitatively analyze the obtained results.

The rest of this document is organized as follows: Sect. 2 introduces Volpara^{TM}, the MRI segmentation and the biomechanical model used for multi-modal registration, Sect. 3 shows the experimental evaluation, while Sect. 5 discusses the main findings of this paper.

2 Methodology

2.1 Volpara^{TM} Density Maps

To compute the spatial distribution of breast glandular tissue from mammograms, we used the commercial software Volpara^{TM}. The basis of Volpara^{TM} software can be found in the work of Highnam et al. [7].

The starting point is to find an area within the mammogram which is entirely adipose (fatty) tissue. This area (P_{fat}) is used as a reference level to compute the thickness of glandular tissue (h_d) at each pixel (x, y) of the mammogram. The

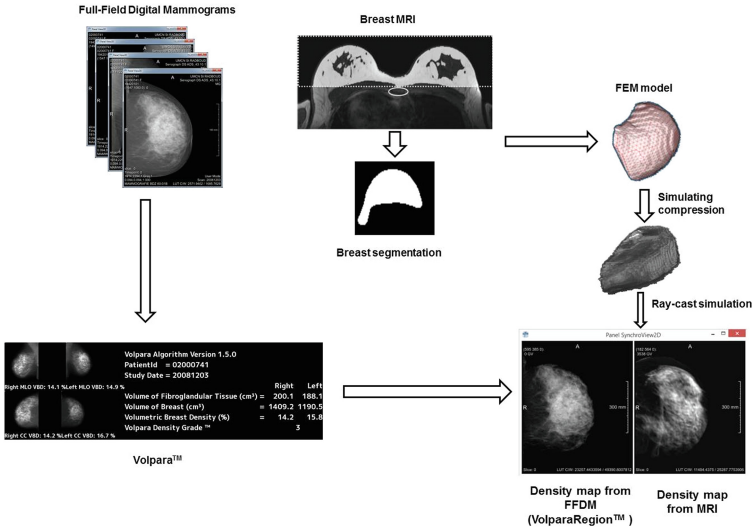

Fig. 1. Scheme of the process to generate the density maps. On the left, from the mammography using the Volpara^{TM} software, while on the right, departing from the MRI.

density map has a resolution equal to 638×765 pixels (0.28×0.28 millimeters per pixel).

In addition to local measures, Volpara^{TM} computes the volume of the glandular tissue, integrating the $h_d(x, y)$ values over the entire mammogram, the breast volume, using the area of the mammogram and the recorded breast thickness, and finally, the breast density and the Volpara Density Grade (VDG), a value, between 1 and 4, comparable to the BI-RADS rating for global breast density [3].

2.2 Generating the Density Map from MRI

In order to generate a density map from breast MRI comparable with the one provided by Volpara^{TM}, the acquisition conditions observed in mammography have to be reproduced. Figure 1 shows the scheme of the process to generate a density map. Firstly, each breast is separated from the rest of the body in the MRI volume. Subsequently, the breast is represented as a 3D model which is compressed simulating the mammographic acquisition and finally projected into a 2D plane using a ray-casting approach. This final projection is the density map obtained from the MRI.

Segmentation. Firstly, image inhomogeneities are corrected using the N4 bias field correction algorithm [15]. The 3D breast MR volume is segmented from the background and separated from the rest of the body using a probabilistic Atlas approach, a methodology similar to the one presented by Gubern-Mérida et al. [5].

Subsequently, internal tissues are further segmented using the FCM [2] and the EM algorithms. We complete this information using two methods that incorporate spatial prior information into them: the Kernelized Fuzzy C-means [17] and the Markov Random Fields, which provides spatial consistency to the Gaussian model. The main reason to use these two algorithms is to avoid the misclassification of skin voxels and uncorrected bias field regions close to the pectoral muscle. Finally, the membership of the voxel to belong to the glandular tissue class is stored, as a 3D density-probabilistic map of the whole MRI volume.

Mammographic Acquisition Simulation. The breast surface mesh and a secondary mesh, belonging to the glandular tissue (voxels with membership higher than 0.5), are extracted from the MR images by means of the marching cubes algorithm. Previously, a morphological operation closes the internal tissue, avoiding small isolated regions within the biomechanical breast model. The tetrahedral mesh is extracted using the open-source package tetgen [13], getting a high number of elements (approx. $100,000$).

The stress-strain relationship is approximated by a nearly incompressible, isotropic and hyperelastic neo-Hookean model for each tissue, using the corresponding Young's modulus measured by Wellman [16] (adipose tissue $E_{fat} = 4.46\,\text{kPa}$ and glandular tissue $E_{gland} = 15.1\,\text{kPa}$ at $Strain = 0.0$ [14]). The breast-body interface is fitted to a linear surface and the nodes belonging to this surface are allowed to slide in the parallel direction to the compression paddle displacement [6]. The simulation is performed by means of the software NiftySim v.2.3.1 [10], using a frictionless contact model to simulate the compression paddle. The necessary information to reproduce the mammographic acquisition (breast thickness, view angle, source-to-detector distance, etc.) is extracted from the DICOM header of the corresponding mammogram.

Finally, a ray-casting algorithm [12], accelerated by a GPU implementation, is used in conjunction with the compressed breast model, to simulate the mammographic geometry. The amount of glandular tissue traversed by each X-ray photon at different locations of the receptor is computed as the length of the ray multiplied by the membership of the traversed voxel.

2.3 Image Registration

After getting the compressed breast image, the biomechanical model is displaced to align as much as possible both density maps, using a Hill-Climbing optimization algorithm (3D/2D registration). The optimization process consists in finding the maximum Dice overlap coefficient between the real mammogram and the projected one. This map is the one that will be quantitatively compared to the map obtained with the Volpara^{TM} software.

3 Experimental Results

3.1 DataSet

The dataset used was acquired at the Radboud University Medical Centre (Nijmegen, The Netherlands) between April 2005 and September 2009, and contains 40 pre-contrast T1 MR images and 80 CC mammograms from 40 women. Patients were selected according to their VDG, choosing 10 patients for each density class. The 40 patients were aged 29 to 59 (mean: 40.91 ± 8.57).

The MRI scanner used was a 1.5 Tesla Siemens scanner (Magnetom Vision, Magnetom Avanto and Magnetom Trio) with dedicated breast coil (CP Breast Array, Siemens, Erlangen). Regarding the mammographic device, the images were acquired by either a GE Senographe 2000D or GE Senographe DS, according to the standard clinical settings. Both studies were acquired in the same day.

3.2 Results

To evaluate our result, each density class is taken independently. Moreover, the parameter of the FCM was set to 2 based on our initial experiments.

Global and local measures are combined to evaluate the agreement between the density maps. On one hand, global measures consist in computing the mutual information (MI) between both density maps and the distance between density maps histograms. On the other hand, local measures were obtained computing the statistics (mean and entropy) of the density maps difference.

Figure 2 shows the results obtained when computing the mutual information between Volpara density maps and the ones obtained from the MRI detailed for each density class and when using the four segmentation algorithms: Fuzzy C-means (FCM), Gaussian mixture models (EM), Kernelized FCM (KFCM) and Markov Random Fields (EM+MRF). We can see that the mutual information measure is higher in denser classes. Moreover, the performance is similar for all

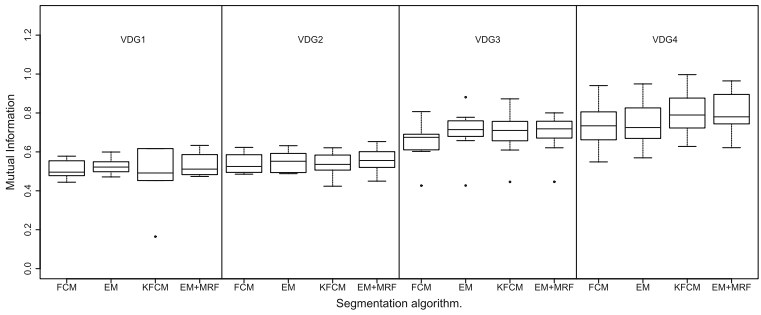

Fig. 2. Mutual information between histograms detailed for each density class (ordered in increasing density class). Higher values indicate a better agreement between the maps.

the algorithms, although adding spatial information provides better results in the densest class.

The histogram of the density maps allows to measure, in a global way, the amount of glandular tissue traversed by the X-ray beam during the projection. Due to the optimization performed we expected the density maps obtained from the mammogram (Volpara^{TM}) and from the MRI to be similar. Figure 3 shows the Euclidean distance between them. According to this measure, EM seems to perform better than FCM, specially in fatty breasts. Spatial information does not provide a significant increase of the algorithms performance.

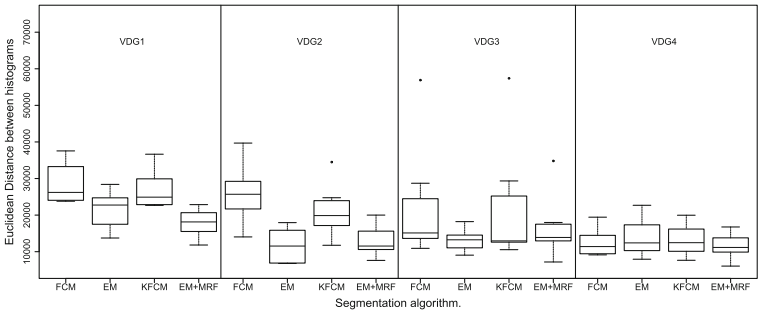

Fig. 3. Euclidean distance between histograms detailed for each density class. Lower values indicate a better agreement between the maps.

Finally, we calculate the point-to-point differences between density maps in order to extract local information of the divergences. In general, statistics extracted from the difference maps show a high similarity between results. For instance, the results of the mean of the difference density maps are shown in Fig. 4. We also observed that the entropy of the difference of the density maps decreases for denser breasts. Regarding algorithms, FCM performs better than EM according to this measure, although the use of spatial information helps to minimize the differences, increasing drastically the performance of the EM algorithm.

4 Discussion

Local distribution and the pattern of glandular tissue provide information to radiologist for risk assessment in localized areas. Comparing those measures from different image modalities (MRI and X-ray mammography) could help to improve the co-localization of these areas in a 3D-space. Our results show a high similarity between the amount of glandular tissue computed from each modality.

Comparing the intensity-based segmentation algorithms used on MRI, the Gaussian mixture model provided better results according to the global criteria while provided worse results according to the local measures. This is mainly

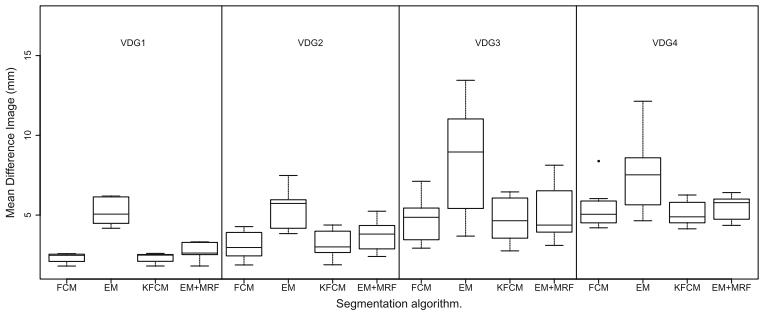

Fig. 4. Mean of the difference density maps detailed for each density class. Lower values indicate a better agreement between the maps.

due to inaccuracies introduced during the multi-modal registration. Moreover, our experiments have shown that the spatial information aids the segmentation and improves the obtained density maps. We also observed that the N4 MRI bias-field correction provided better results in denser breasts.

5 Conclusions

In this paper we analyzed the impact of four tissue segmentation algorithms during the multi-modal registration of breast MRI to X-ray mammography. Two of them consider only the gray intensity levels in the images while the others incorporated spatial information to improve segmentation results. The density maps obtained from this registration are then quantitatively compared with the corresponding maps obtained from the Volpara^{TM} software in the full-field digital mammograms.

Results show a high agreement between density maps. However, inaccuracies during the registration or the over-/underestimation of glandular tissue for each voxel reduce the accuracy of results. Further work will include a more robust multi-modal registration approach.

Acknowledgement. This research has been partially supported from the Ministry of Economy and Competitiveness of Spain, under project references TIN2012-37171-C02-01 and DPI2015-68442-R, and the FPI grant BES-2013-065314.

References

1. Baluwala, H., Sanghani, P., Malcom, D., Nielsen, P., Nash, M.: Comparison of fibroglandular tissue segmentation algorithms in breast MRI. In: Harz, M. et al. (ed.) Workshop MICCAI Breast Image Analysis, pp. 105–112 (2015)
2. Bezdek, J., Pal, M., Keller, J.: Fuzzy Models and Algorithms for Pattern Recognition and Image Processiong. Kluwer Academic Publishers, Dordrecht (1999)

3. Damases, C., Brennan, P., Mello-Thoms, C., McEntee, M.: Mammographic breast density assessment using automated volumetric software and breast imaging reporting and data system (BIRADS) categorization by expert radiologist. Acad. Radiol. **23**(1), 70–77 (2015)
4. Dietzel, M., Hopp, T., Ruiter, N., Zoubi, R., Runnebaum, I.B., Kaiser, W.A., Baltzer, P.A.T.: Fusion of dynamic contrast-enhanced magnetic resonance mammography at 3.0T with X-ray mammograms: pilot study evaluation using dedicated semi-automatic registration software. Eur. J. Radiol. **79**(2), 98–102 (2011)
5. Gubern-Mérida, A., Kallenberg, M., Platel, B., Mann, R., Martí, R., Karssemeijer, N.: Volumetric breast density estimation from full-field digital mammograms: a validation study. PLoS One **9**(1), e85952 (2014)
6. Han, L., Hipwell, J., Tanner, C., Taylor, Z., Mertzanidou, T., Cardoso, J., Ourselin, S., Hawkes, D.: Development of patient-specific biomechanical models for predicting large breast deformation. Phys. Med. Biol. **57**(2), 455–472 (2012)
7. Highnam, R., Brady, S.M., Yaffe, M.J., Karssemeijer, N., Harvey, J.: Robust breast composition measurement - Volpara^{TM}. In: Martí, J., Oliver, A., Freixenet, J., Martí, R. (eds.) IWDM 2010. LNCS, vol. 6136, pp. 342–349. Springer, Heidelberg (2010)
8. Hopp, T., Ruiter, N.V.: 2D/3D registration for localization of mammographically depicted lesions in breast MRI. In: Maidment, A.D.A., Bakic, P.R., Gavenonis, S. (eds.) IWDM 2012. LNCS, vol. 7361, pp. 627–634. Springer, Heidelberg (2012)
9. Hopp, T., Duric, N., Ruiter, N.: Image fusion of ultrasound computer tomography volumes with X-ray mammograms using a biomechanical model based 2D/3D registration. Comput. Med. Imaging Graph **40**, 170–181 (2015)
10. Johnsen, S., Taylor, Z.A., Clarkson, M., Hipwell, J., Modat, M., Eiben, B., Han, L., Hu, Y., Mertzanidou, T., Hawkes, D.J., Ourselin, S.: NiftySim: a GPU-based nonlinear finite element package for simulation of soft tissue biomechanics. J. Comput. Assist. Radiol. Surg. **10**(7), 1077–1095 (2014)
11. Malur, S., Wurdinger, S., Moritz, A., Michels, W., Schneider, A.: Comparison of written reports of mammography, sonography and magnetic resonance mammography for preoperative evaluation of breast lesions, with special emphasis on magnetic resonance mammography. Breast Cancer Res. **3**(1), 55–60 (2001)
12. Roth, S.: Ray casting for modeling solids. Comput. Graph. Image Process. **18**(2), 109–144 (1982)
13. Si, H.: Tetgen, a Delaunay-based quality tetrahedral mesh generator. ACM Trans. Math. Softw. **41**(2), 1–36 (2015)
14. Tanner, C., Degenhard, A., Schnabel, J., Smith, A.C., Hayes, C., Sonoda, L., Lach, M., Hose, D., Hill, D., Hawkes, D.: A method for the comparison of biomechanical breast models. IEEE Workshop MMBIA **2001**, 11–18 (2001)
15. Tustison, N., Avants, B., Cook, P., Zheng, Y., Egan, A., Yushkevich, P., Gee, J.: N4ITK: improved N3 bias correction. IEEE Trans. Med. Imaging **29**(6), 1310–1320 (2010)
16. Wellman, P.: Tactile imaging. Ph.D. thesis, Cambridge, MA, Harvard University's Division of Engineering and Applied Sciences (1999)
17. Wu, Z., Xies, W., Yu, J.: Fuzzy C-means clustering algorithm based on kernel method. In: Proceedings Fifth International Conference on Computational Intelligence and Multimedia Applications, ICCIMA 2003, pp. 49–54. IEEE (2003)